Macromolecular Bioscience
www.mbs-journal.de

Preventive Effects of Thermosensitive Biopolymer-Conjugated C-Peptide against High Glucose-Induced Endothelial Cell Dysfunction

*Se-Hui Jung, Jee-Yeon Lee, Seong-Hyeon Lee, Mi-Hye Kwon, Eun-Taek Han, Won Sun Park, Seok-Ho Hong, Young-Myeong Kim, and Kwon-Soo Ha**

C-peptide has emerged as a potential drug for treating diabetic complications. However, clinical application of C-peptide is limited by its short half-life during circulation and costly synthesis methods. To overcome these limitations, a biocompatible and thermosensitive biopolymer-C-peptide conjugate composed of human C-peptide genetically conjugated at the C-terminus of nine repeats of lysine-containing elastin-like polypeptide (K9-C-peptide) is generated. K9-C-peptide exhibits reversible thermal phase behavior with a transition temperature dependent on polypeptide concentration. Degradation of K9-C-peptide hydrogel depends on the concentration of four cleavage enzymes as well as the reaction time and frequency of treatments with elastase-2. The preventive effect of K9-C-peptide against high glucose-induced human aortic endothelial cell dysfunction is further investigated. K9-C-peptide inhibits high glucose-induced intracellular reactive oxygen species generation, transglutaminase 2 activation, and apoptosis, similar to the inhibitory effects of human C-peptide. Thus, K9-C-peptide is a potential drug depot for the sustained delivery of C-peptide to treat diabetic complications.

1. Introduction

Chronic hyperglycemia and subsequent metabolic changes in diabetes mellitus result in micro- or macrovascular complications leading to diabetes-related morbidity and mortality through progressive blood vessel damage and dysfunction.[1] Recent studies report that diabetic vasculopathy is predominantly caused by apoptosis due to elevated intracellular reactive oxygen species (ROS) levels and consequent transglutaminase 2 (TGase2) activation.[2] Glycemic control by administration of insulin or antihyperglycemic drugs is the primary approach to preventing diabetic complications.[1] However, treatment based on glycemic control alone is not effective for preventing long-term diabetic complications, and alternative therapeutic strategies are still needed to ameliorate diabetes-mediated organ damage.[3]

Proinsulin C-peptide has emerged as an attractive potential drug for treating diabetic complications because numerous reports show beneficial effects of C-peptide against diabetic vasculopathy, including diabetic retinopathy, neuropathy, nephropathy, vascular dysfunctions, and impaired wound healing.[1,2,4–8] C-peptide consisting of 31 amino acids is cleaved from proinsulin and secreted into the circulation from pancreatic β-cells in equimolar concentrations with insulin.[9] Normalization of blood C-peptide level in type 1 diabetic mice prevents hyperglycemia-induced vascular dysfunction by suppressing endothelial apoptosis through inhibiting hyperglycemia-induced ROS generation and TGase2 activation.[2,8,10] Supplementation with C-peptide prevents hyperglycemia-induced vascular leakage and metastasis in the lungs of diabetic mice.[9] Also, local administration of C-peptide into the vitreous chamber of type 1 diabetic mice prevents diabetic retinopathy by inhibiting hyperglycemia-induced ROS generation and TGase2 activation.[6,11]

However, the clinical application of C-peptide for treating diabetic complications is limited for two reasons. First, C-peptide has a short circulating half-life of about 30 min due to its rapid renal clearance and degradation by enzymatic reactions,[12] suggesting that repeated administration of C-peptide several times daily is required to maintain an effective blood C-peptide level. To lengthen the half-life of C-peptide, Wahren et al. prepared a long-acting form of C-peptide by chemical conjugation with polyethylene glycol (PEG),[13,14] which is one

Dr. S.-H. Jung, J.-Y. Lee, S.-H. Lee, Dr. M.-H. Kwon, Prof. Y.-M. Kim, Prof. K.-S. Ha
Department of Molecular and Cellular Biochemistry
Kangwon National University School of Medicine
Chuncheon, Kangwon-Do 200-701, Korea
E-mail: ksha@kangwon.ac.kr
Prof. E.-T. Han
Department of Medical Environmental Biology and Tropical Medicine
Kangwon National University School of Medicine
Chuncheon, Kangwon-Do 200-701, Korea
Prof. W. S. Park
Department of Physiology
Kangwon National University School of Medicine
Chuncheon, Kangwon-Do 200-701, Korea
Prof. S.-H. Hong
Department of Internal Medicine
Kangwon National University School of Medicine
Chuncheon, Kangwon-Do 200–701, Korea
The ORCID identification number(s) for the author(s) of this article can be found under https://doi.org/10.1002/mabi.201900129.

DOI: 10.1002/mabi.201900129

of the most commonly used approaches for prolonged drug delivery. Administration of PEGylated C-peptide twice a week for 20 weeks into type 1 diabetic patients is more effective than administration of native C-peptide[14]; however, the long-term circulation of PEG molecules can trigger unwanted effects, including immune responses, and the in vivo behavior of conjugates cannot be controlled due to polydispersity of the polymer and poorly controlled stoichiometry.[15] Second, C-peptide is mostly produced by chemical synthesis, which is costly.

Thermosensitive elastin-like polypeptides (ELPs) are a class of recombinant biopolymers that are useful for controlled drug delivery.[16] ELPs are inspired by human elastin and composed of a repeated pentapeptide motif (VPGXG).[17] The physicochemical properties of ELPs, such as their thermosensitive sol-gel transition, ensure spatiotemporally controlled release of drugs and allow chromatography-free purification of conjugated proteins or peptides.[18] The temperature-enabled sol-gel transition is easily tuned by modifying the number and sequence of ELP units. Furthermore, genetic conjugation of ELPs with proteins or peptides using recombinant DNA technology permits the tight control of physicochemical properties and stoichiometry between proteins and polymers. ELPs genetically conjugated with drugs have been used for treatment of diseases including cancer, type 2 diabetes, osteoarthritis, and neuroinflammation by forming drug depots or self-assembled nanoparticles.[19–22]

In this study, we designed a human C-peptide conjugated at the C-terminus of nine repeats of lysine-containing ELPs (K9-C-peptide) to allow sol-gel transition below body temperature (**Figure 1**A). We successfully prepared K9-C-peptide through recombinant DNA technology, *E. coli* expression, and inverse transition cycling (ITC) (Figure 1B). This K9-C-peptide exhibited reversible thermal phase behavior, and the gel was cleaved by four cleavage enzymes. We applied this K9-C-peptide to investigate its preventive effect against high glucose-induced intracellular events in human aortic endothelial cells (HAECs). K9-C-peptide inhibited glucose-induced intracellular ROS generation and TGase2 activation in a dose-dependent manner, similar to the inhibitory effects of human C-peptide. High glucose-induced apoptosis was blocked by K9-C-peptide and human C-peptide. Therefore, K9-C-peptide successfully suppressed hyperglycemia-mediated dysfunction of endothelial cells and is a potential drug depot for sustained delivery of C-peptide.

A

ELP analogues	Amino acid sequence
K8	$[(VPGVG)_{11}(VPGKG)_1(VPGVG)_1]_8$
K9-C-peptide	$[(VPGVG)_{11}(VPGKG)_1(VPGVG)_1]_9$DPNYPRGHEAEDLQV GQVELGGGPGAGSLQPLALEGSLQ

Elastin unit, VPGVG; lysine-substituted elastin unit, (VPGKG); linker, DPNYPRGH; C-peptide sequence, EAEDLQVGQVELGGGPGAGSLQPLALEGSLQ

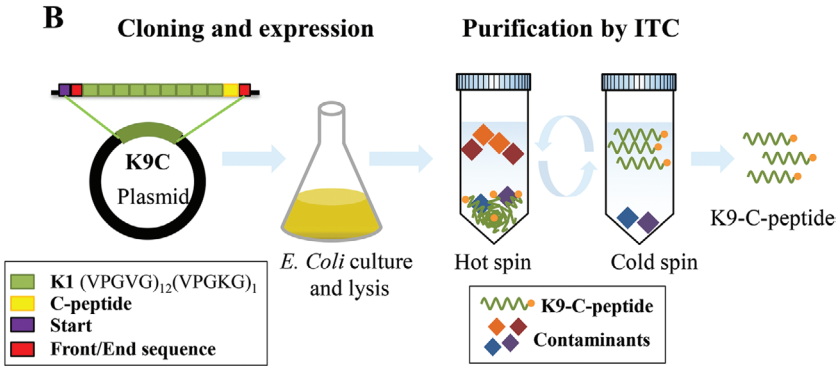

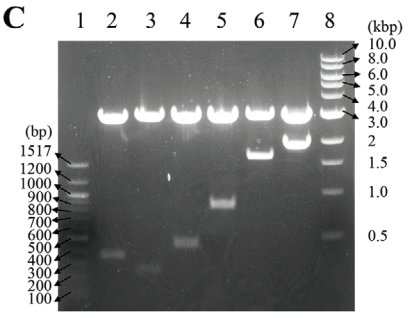

Figure 1. Amino acid sequence and preparation of K9-C-peptide. A) Amino acid sequences of K8 and K9-C-peptide. B) Schematic diagram of K9-C-peptide expression and purification. C) Visualization of genes encoding K8 and K9-C-peptide constructed by recursive directional ligation. 1: DNA ladder (bp). 2: K1-C-peptide. 3, 4, 5, and 6: genes for K1, K2, K4, and K8, respectively. 7: K9-C-peptide. 8: DNA ladder (kbp).

2. Experimental Section

2.1. Chemical Reagents

3-Aminopropyltrimethoxysilane, pepsin, and trypsin were obtained from Sigma-Aldrich (St. Louis, MO). Elastase-2 from leucocytes of purulent human sputum was purchased from Elastin Products Company (Owensville, MO). Collagenase-2 was obtained from Worthington Biochemical Corporation (Lakewood, NJ). Cy3 mono N-hydroxysuccinimide (NHS)-ester and Biospin columns were purchased from GE Healthcare (Little Chalfont, UK) and Bio-Rad (Hercules, CA), respectively. Polydimethylsiloxane solution was obtained from Sewang Hitech (Gimpo, Korea).

2.2. Construction of Plasmids for K8 and K9-C-Peptide Production

Synthetic genes encoding K1 $[(VPGVG)_{11}(VPGKG)_1(VPGVG)_1]$ ELP and K1-conjugated human C-peptide (K1-C-peptide) containing a cleavable linker sequence, DPNYPRGH, were synthesized (Macrogene, Seoul, Korea) and ligated into a pBSC (KS+) vector. Using a synthetic recursive directional ligation strategy, the gene encoding an ELP consisting of eight repeats of K1 was generated

as shown in Figure 1A. The gene encoding K8 was fused at the 5′-end to the gene encoding K1-C-peptide. The resulting gene for K9-C-peptide was inserted into the pET25b+ vector for polypeptide expression. All completed constructs were confirmed by DNA sequencing.

2.3. Peptide Expression and Purification

For preparation of K8 and K9-C-peptide, expression vectors encoding K8 and K9-C-peptide were transformed into *E. coli* strain BL21 (DE3), and expression and ITC were performed as previously described.[23] Briefly, transformed cells were grown at 37 °C to an OD_{600} of 0.4–0.6 after induction with 1 mmol L^{-1} isopropyl β-D-1-thiogalactopyranoside for 4 h at 37 °C. Bacterial cells were harvested by centrifugation for 10 min at 12 000 g at 4 °C, resuspended in phosphate-buffered saline [PBS; 8.1 mmol L^{-1} Na_2HPO_4, 1.2 mmol L^{-1} KH_2PO_4, 138 mmol L^{-1} NaCl, 2.7 mmol L^{-1} KCl (pH 8.0)], and sonicated for 30 pulses of 10 s each on ice. DNA and insoluble fractions were precipitated by centrifugation at 4 °C for 15 min at 18 000 g after incubation with 10% polyethyleneimine for 30 min on ice. NaCl was added to the soluble fractions (final concentration 3 mol L^{-1}) and incubated for 10 min at 50 °C. The turbid suspensions were centrifuged at 50 °C for 15 min at 18 000 g (hot spin). The supernatants were removed, and the pellets were suspended in chilled PBS on ice. The resulting solutions were centrifuged at 4 °C for 10 min at 18 000 g, and the supernatants were reserved (cold spin). This ITC process was repeated to yield purified products. The resulting supernatants were dialyzed against milli-Q water for 24 h and lyophilized.

2.4. In Vitro Characterization of K9-C-Peptide

To confirm production and purification of K9-C-peptide, samples collected from each ITC process were loaded onto a 10% polyacrylamide gel. Following electrophoresis, the gel was stained with Coomassie blue dye and imaged using a ChemiDoc scanner.

To characterize the inverse transition temperature of K9-C-peptide, the turbidity of 2.5–100 μmol L^{-1} K9-C-peptide solutions in PBS was monitored at a wavelength of 350 nm as a function of temperature at a heating rate of 1 °C min^{-1} on a SpectraMax M5 Multi-Mode microplate reader (Molecular Devices, Sunnyvale, CA).

2.5. Conjugation of K9-C-Peptide with Cy3 NHS Ester

K9-C-peptide was labeled with Cy3 NHS ester as previously reported.[24] Briefly, 1 mL of each 20 mg mL^{-1} K9-C-peptide solution in 100 mmol L^{-1} sodium bicarbonate buffer (pH 8.3) was mixed with 13 μL of 5 mg mL^{-1} Cy3 mono NHS ester in 10% dimethyl sulfoxide and incubated for 2 h on ice. To quench the reaction, 50 μL of 1 mol L^{-1} Tris-HCl (pH 8.0) was added to the reaction solution. Reaction mixture was loaded onto 1.5-mL Sephadex G-25 columns, and Cy3-conjugated K9-C-peptide was eluted by centrifugation for 3 min at 1050 g.

2.6. On-Chip Degradation Profiling of K9-C-Peptide Hydrogel

Amine-modified glass slides were prepared as previously reported.[25] Briefly, glass slides (75 mm × 25 mm) were cleaned with a $H_2O_2/NH_4OH/H_2O$ (1:1:5, v/v) solution, immersed in 95% ethanol with 1.5% (v/v) 3-aminopropyltrimethoxysilane for 2 h, and baked overnight at 110 °C. Well-type amine arrays were fabricated by mounting polydimethylsiloxane gaskets onto the amine-modified glass slides.[26]

The enzymatic degradation profiling of K9-C-peptide using four cleavage enzymes including collagenase-2, elastase-2, pepsin, and trypsin was carried out (n = 3) as previously reported.[27] Briefly, a 10 mg mL^{-1} aliquot of Cy3-conjugated K9-C-peptide was applied to the well-type amine arrays for 2 h at 40 °C to allow hydrogel formation. The arrays were incubated for 2 h at 37 °C with the indicated concentrations of collagenase-2 in buffer A (50 mmol L^{-1} Tris-HCl, 150 mmol L^{-1} NaCl, 5 mmol L^{-1} $CaCl_2$, 0.2 mmol L^{-1} NaN_3, and 0.002% Brij-35, pH 7.6), elastase-2 in buffer B (100 mmol L^{-1} Tris-HCl and 100 mmol L^{-1} NaCl, pH 7.5), pepsin in buffer C (10 mmol L^{-1} HCl, pH 2.0), or trypsin in buffer D (50 mmol L^{-1} Tris-HCl, 20 mmol L^{-1} $CaCl_2$, and 0.02% Tween-20, pH 8.1). The arrays were washed with Tris-buffered saline (50 mmol L^{-1} Tris-HCl, pH 7.5, and 140 mmol L^{-1} NaCl) containing 0.1% Tween-20 for 10 min and then with Milli-Q water for 5 min, dried under air, and analyzed using a confocal microscope equipped with a motorized sample stage (K1-Fluo; Nanoscope Systems, Taejon, Korea). The amount of K9-C-peptide remaining on the array surface was calculated using a standard curve, which was plotted as the sigmoidal fit using the Origin program, as follows:

$$x = \log x_0 - \left(\log\left(\frac{A_2 - A_1}{y - A_1} - 1 \right) \Big/ P \right) \quad (1)$$

where x represents the K9-C-peptide concentration; x_0 represents the K9-C-peptide concentration at half maximal fluorescence intensity; A_1 and A_2 represent the upper and lower asymptotes, respectively; y represents sample fluorescence intensity and P represents power. The half-maximal effective concentrations (EC_{50}) for cleavage enzymes were calculated by the following modified Langmuir isotherm using GraphPad PRISM8 (GraphPad Software; San Diego, CA):

$$F_{obs} = (F_{max} \times [\text{enzyme}] / EC_{50} + [\text{enzyme}]) + \text{background} \quad (2)$$

where F_{obs} is the fluorescence intensity of triplicate spots, F_{max} is the maximum fluorescence at saturation, [enzyme] is the enzyme concentration, and EC_{50} is the apparent half-maximal effective concentration. The enzyme concentration of each protease was expressed as U mL^{-1} as defined in the manufacturer's instructions as follows: one unit of collagenase-2 liberates 1 μmol L-leucine-equivalent from collagen for 5 h (pH 7.5 at 37 °C), one unit of elastase-2 hydrolyzes 1 mmol MeO-Suc-APV-pNA per min (pH 7.5 at 25 °C), one unit of pepsin liberates the amount of Tyr producing an increase in the absorbance of 0.001 min^{-1} at 280 nm (pH 2 at 37 °C), and one unit of trypsin cleaves the amount of benzoyl L-arginine ethyl ester producing an increase in the absorbance of 0.001 min^{-1} at 253 nm (pH 7.6 at 25 °C).

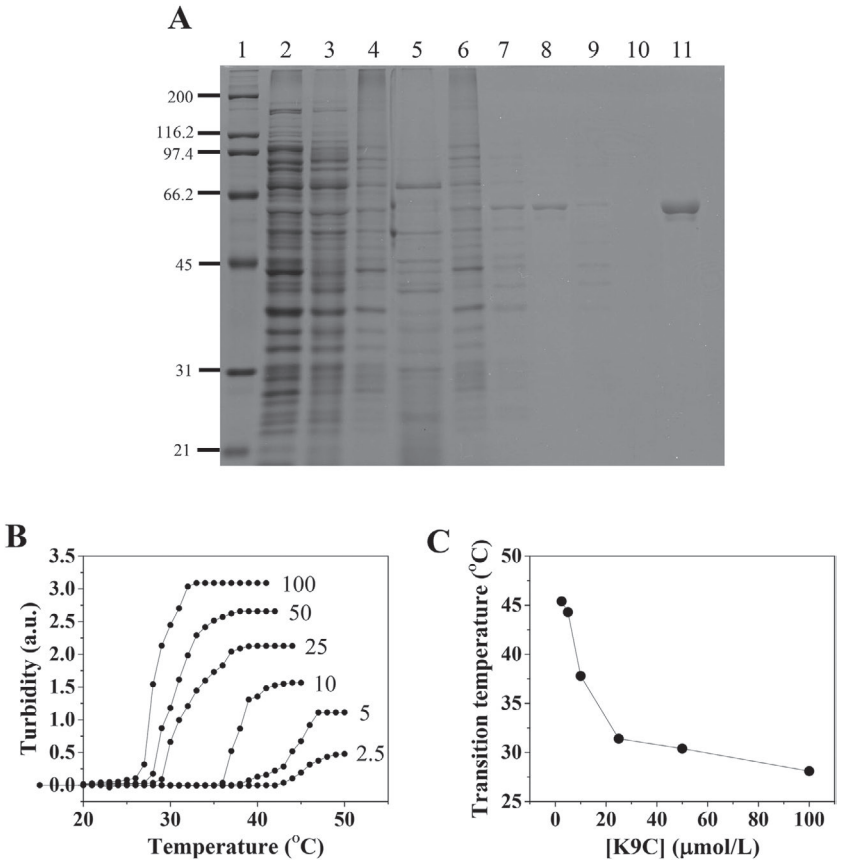

Figure 2. In vitro characterization of K9-C-peptide. A) Coomassie-stained SDS-PAGE for visualizing the size and purity of K9-C-peptide purified by ITC. 1: MW ladder (kDa). 2: Crude lysate. 3: Soluble fraction following DNA precipitation. 4 and 5: pellet and supernatant after first hot spin, respectively. 6 and 7: pellet and supernatant after first cold spin, respectively. 8 and 9: pellet and supernatant after second hot spin, respectively. 10 and 11: pellet and supernatant after second cold spin, respectively. B) Turbidity profiles of concentrations from 2.5 to 10 mmol L^{-1} of K9-C-peptide as a function of solution temperature. Optical density at 350 nm of each solution was measured as a function of temperature at a heating rate of 1 °C min^{-1}. C) Transition temperature as a function of H9C concentration.

2.7. Cell Culture and Treatment

HAECs were purchased from PromoCell (Heidelberg, Germany) and grown on 2% gelatin-coated plates in M199 medium supplemented with 20% fetal bovine serum, 3 ng mL^{-1} basic fibroblast growth factor, 5 U mL^{-1} heparin, 100 U mL^{-1} penicillin, and 100 mg mL^{-1} streptomycin in a humidified 5% CO_2 incubator. For experiments, HAECs were incubated for 6 h in low-serum medium supplemented with 2% fetal bovine serum, 0.1 ng mL^{-1} basic fibroblast growth factor, and antibiotics and then treated with 30 mmol L^{-1} D-glucose.

2.8. Measurement of Intracellular ROS and TGase Activity Levels

Intracellular ROS level was measured using 2′,7′-dichlorodihydrofluorescein diacetate (H_2DCFDA) (ThermoFisher Scientific, Waltham, MA) as described previously.[9] HAECs were incubated with the indicated concentrations of human C-peptide, K8, or K9-C-peptide for 30 min and treated with 10 μmol L^{-1} H_2DCFDA for 10 min. Labeled cells were analyzed immediately using confocal microscopy (K1-Fluo). Single-cell fluorescence intensities were determined for 30 randomly selected cells/experiment. Intracellular ROS was determined by comparing the fluorescence intensities of treated cells with those of control cells ($n = 3$).

Intracellular TGase activity was determined by measuring incorporated 5-(biotinamido)pentylamine (BAPA) into cells as previously reported.[11] HAECs were pretreated with the indicated concentrations of human C-peptide, K8, or K9-C-peptide for 30 min and treated with 1 mmol L^{-1} BAPA for 60 min. Incorporated BAPA in cells mediated by TGase2 was probed with FITC-conjugated streptavidin (1:200; MilliporeSigma, Burlington, MA) for 1 h after fixation and permeabilization of cells. The fluorescence intensities of stained cells were determined by confocal microscopy (K1-fluo) for 30 randomly selected cells/experiment ($n = 3$).

2.9. Evaluating Cytotoxicity of C-Peptide Derivatives

The cytotoxicity of C-peptide derivatives was evaluated by MTT assay as previously reported.[2] HAECs were cultured on a 24-well plate and treated with the indicated concentrations of human C-peptide, K8, or K9-C-peptide for 24 h. After replacement of culture medium with fresh medium, 200 μL of 1 mg mL^{-1} 3-(4, 5-dimethylthiazolyl-2)-2,5-diphenyltetrazolium bromide solution was added to each well and incubated for 4 h. Resulting formazan crystals were dissolved in dimethyl sulfoxide, and the absorbance of each well was obtained at 570 nm ($n = 3$).

2.10. Measurement of Apoptosis

Apoptotic cells were detected by terminal deoxynucleotidyl transferase dUTP nick end labeling (TUNEL) assay using an APO-BrdU TUNEL assay kit (BD Bioscience, San Jose, CA) as described previously.[2] Briefly, cells were fixed for 20 min with 1% (w/v) paraformaldehyde in PBS followed by treatment for 30 min with 70% (v/v) ethanol on ice. Fixed cells were incubated for 1 h at 37 °C with a DNA-labeling solution containing terminal deoxynucleotidyl transferase and 5-bromo-2-deoxyuridine in reaction buffer. Cells were then incubated with FITC-labeled 5-bromo-2-deoxyuridine antibody for 30 min and 1 μg mL^{-1} DAPI for 10 min. Mounted cells were visualized using confocal microscopy (K1-Fluo). The ratio of apoptotic cells in total cells were calculated from three independent experiments ($n = 3$).

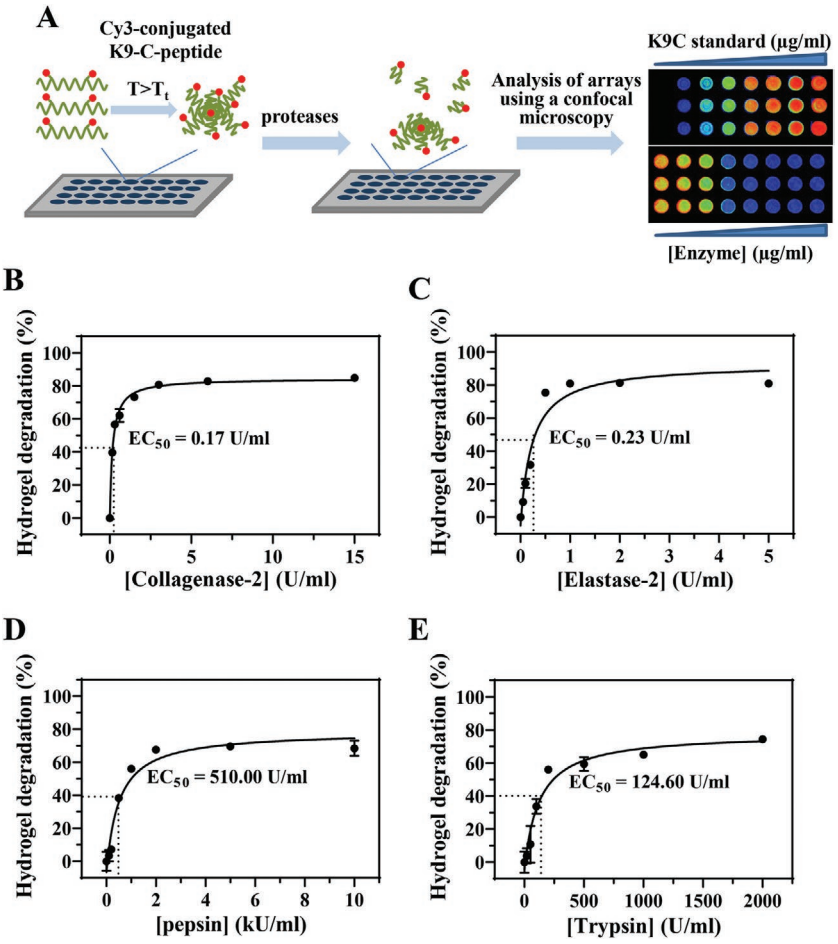

Figure 3. Quantitative analysis of enzymatic degradation of K9-C-peptide by four proteases. A) K9-C-peptide hydrogel arrays were fabricated by immobilizing 10 mg mL^{-1} Cy3-conjugated K9-C-peptide onto well-type amine arrays. Enzyme reaction mixtures containing the indicated concentrations of four proteases including B) collagenase-2, C) elastase-2, D) pepsin, and E) trypsin were applied to the arrays and incubated for 2 h at 37 °C. The resulting arrays were analyzed using motorized confocal microscopy, and the degradation rate of K9-C-peptide hydrogel by four proteases was calculated using a standard curve ($n = 3$). Results are expressed as the mean ± SD from three independent experiments.

2.11. Statistical Analysis

Data are expressed as the mean ± standard deviation (SD) of at least three independent experiments and were analyzed using OriginPro 2015 software (OriginLab, Northampton, MA). The statistical significance of differences between groups was determined using unpaired Students *t*-tests. A *P* value less than 0.05 was considered statistically significant.

3. Results

3.1. Preparation and Characterization of K9-C-Peptide

The gene encoding K8, composed of eight repeats of lysine-containing ELPs (ELP-$V_{12}K_1$), was prepared using a seamless cloning strategy based on synthetic recursive directional ligation and further fused at the 5′-end of the gene encoding K1-C-peptide (Figure 1A,B). Genes obtained by each round of recursive directional ligation (K1, K2, K4, and K8) and by fusion of K8 with K1-C-peptide were visualized by agarose gel electrophoresis after double-digestion with BamHI and HindIII (Figure 1C). The sequences of K8 and K9-C-peptide genes were confirmed by DNA sequencing (data not shown).

K8 and K9-C-peptide were purified from *E. coli* using ITC with yields of 10 mg L^{-1} culture (data not shown). SDS-PAGE was used to determine the purity and molecular weight of K9-C-peptide (**Figure 2**A). Samples retained throughout the ITC process were visualized on a Coomassie-stained SDS-PAGE gel, and a 60-kDa band protein was identified as a K9-C-peptide with a calculated molecular weight of 53 kDa. Western blot analysis showed that the 60-kDa band was composed of C-peptide (data not shown). This result demonstrates that K9-C-peptide was successfully purified by ITC and that two cycles of ITC were sufficient for its purification.

The thermal responses of K9-C-peptide were investigated by measuring the turbidity of K9-C-peptide solutions ranging from 2.5 to 100 μmol L^{-1} as a function of temperature. The turbidity of K9-C-peptide solutions increased in a temperature-dependent manner, suggesting that coacervates were formed by sol-gel transition (Figure 2B). The transition temperature of K9-C-peptide solutions decreased from 45.4 to 28.1 °C in a concentration-dependent manner (Figure 2C). These results provide evidence of the successful preparation of K9-C-peptide that can be used as an injectable depot of C-peptide.

3.2. Quantitative Analysis of the Degradation of K9-C-Peptide by Proteases

To visualize and quantitatively analyze the degradation of K9-C-peptide by proteases, Cy3-conjugated K9-C-peptide hydrogel arrays were incubated with the indicated concentrations of four proteases: collagenase-2, elastase-2, pepsin, and trypsin (**Figure 3**A). EC_{50} values for each enzyme were determined by plotting degradation rates based on the amount of Cy3-conjugated K9-C-peptide fragments detached from the array spots against the protease concentrations. All four enzymes increased K9-C-peptide degradation in an enzyme concentration-dependent manner (Figure 3B–F). The resulting EC_{50} values of the four enzymes were 0.17, 0.23, 510.00, and 124.60 U mL^{-1}, respectively. These results demonstrate that collagenase-2 and elastase-2 more efficiently cleaved K9-C-peptide than pepsin and trypsin, consistent with previous reports.[28–31]

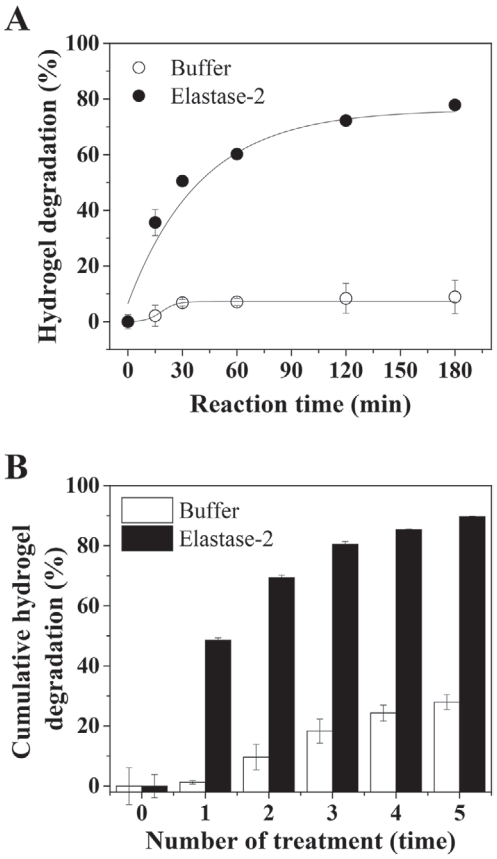

Figure 4. Cumulative K9-C-peptide hydrogel degradation. K9-C-peptide hydrogel degradation with elastase-2 was determined using hydrogel arrays depending on A) incubation time and B) number of treatments. A) Reaction mixtures containing 0.5 U mL^{-1} elastase-2 were applied to the arrays and incubated for the indicated times ($n = 3$). B) Reaction mixture containing 0.5 U mL^{-1} elastase-2 was applied five times to the arrays for 30 min each application ($n = 3$). K9-C-peptide hydrogel degradation (%) was calculated using a confocal microscope. Results are expressed as the mean ± SD from three independent experiments.

To simulate C-peptide release by hydrogel degradation in the presence of proteases, we investigated time-dependent degradation of Cy3-conjugated K9-C-peptide hydrogel using on-chip degradation assay by applying elastase-2 to the hydrogel arrays for the indicated times. Degradation of K9-C-peptide hydrogel by elastase-2 increased in a time-dependent manner, with a maximal degradation of 72.3% at 120 min, whereas reaction buffer alone induced degradation of less than 10% (**Figure 4**A). We next determined the cumulative degradation of Cy3-conjugated K9-C-peptide hydrogel by repeated 30-min elastase-2 treatments. We observed that 48.6 ± 0.8% of the hydrogel was degraded after the first treatment, and hydrogel degradation increased depending on the number of treatments, with maximal degradation (89.7 ± 0.2%) after the fifth treatment (Figure 4B). In the absence of elastase-2, degradation of K9-C-peptide hydrogel increased depending on the number of buffer treatments from 1.3 ± 0.6% (after the first treatment) to 27.9 ± 2.5% (after the fifth treatment), suggesting that repeated washing with detergent-containing buffer induced partial degradation of the hydrogel. These results suggest that C-peptide tethered to ELP hydrogel can be released by blood-circulating proteases, including elastase-2.

3.3. Preventive Effect of K9-C-Peptide against High Glucose-Induced Intracellular ROS Generation, TGase2 Activation, and Apoptosis in HAECs

C-peptide prevents the pathogenesis of diabetic complications by inhibiting hyperglycemia-induced ROS generation, TGase2 activation, and subsequent endothelial apoptosis.[1,2] Thus, we investigated whether K9-C-peptide has similar inhibitory effects as human C-peptide in high glucose-induced intracellular events. We initially studied the cytotoxicity of K9-C-peptide by MTT assay in HAECs. K9-C-peptide showed no cytotoxicity at concentrations ranging from 1 to 5 nmol L^{-1} (**Figure 5**A). Human C-peptide and K8, a negative control biopolymer of K9-C-peptide without C-peptide, also showed no cytotoxicity. Thus, K9-C-peptide is biocompatible and can be used to study the effects of the K9-C-peptide on high glucose-induced intracellular events in HAECs.

High glucose caused an increase in intracellular ROS levels by approximately 2.1-fold, which was prevented by treatment with K9-C-peptide in a concentration-dependent manner, with a maximal effect at 1 nM (Figure 5B,C). Human C-peptide showed a similar inhibitory effect as K9-C-peptide against high glucose-induced ROS generation, but K8 had no inhibitory effect. We next studied the effects of K9-C-peptide and human C-peptide on high glucose-induced TGase2 activation in HAECs. High glucose increased in situ TGase activity by approximately 1.7-fold, which was blocked by transfection with TGM2-specific siRNA (Figure 5D). TGM-2 siRNA suppressed TGase2 protein expression, suggesting that TGase2, but not other TGase family members, predominantly contribute to the high glucose-induced TGase activation in HAECs. Both K9-C-peptide and human C-peptide inhibited high glucose-induced TGase2 activation in a concentration-dependent manner, with a maximal effect at 1 nM, whereas K8 had no effect (Figure 5E).

We next investigated the inhibitory effects of K9-C-peptide and human C-peptide on high glucose-induced endothelial apoptosis by TUNEL staining. High glucose increased the number of TUNEL-positive cells, which was inhibited by both K9-C-peptide and human C-peptide but not by K8 (**Figure 6**A,B). Taken together, our results suggest that K9-C-peptide has similar biological activities as human C-peptide in preventing high glucose-induced apoptosis through inhibiting intracellular ROS generation and TGase2 activation in HAECs.

4. Discussion

In this study, we designed a biocompatible and thermosensitive biopolymer conjugate K9-C-peptide by genetic fusion of C-peptide with lysine-containing ELPs to provide a potential therapeutic avenue for treating diabetic vasculopathy. Proinsulin C-peptide has beneficial effects against diabetic complications. However, its clinical application for treating diabetic complications is impeded due to its short circulation time and costly synthesis methods. To address these issues, we prepared

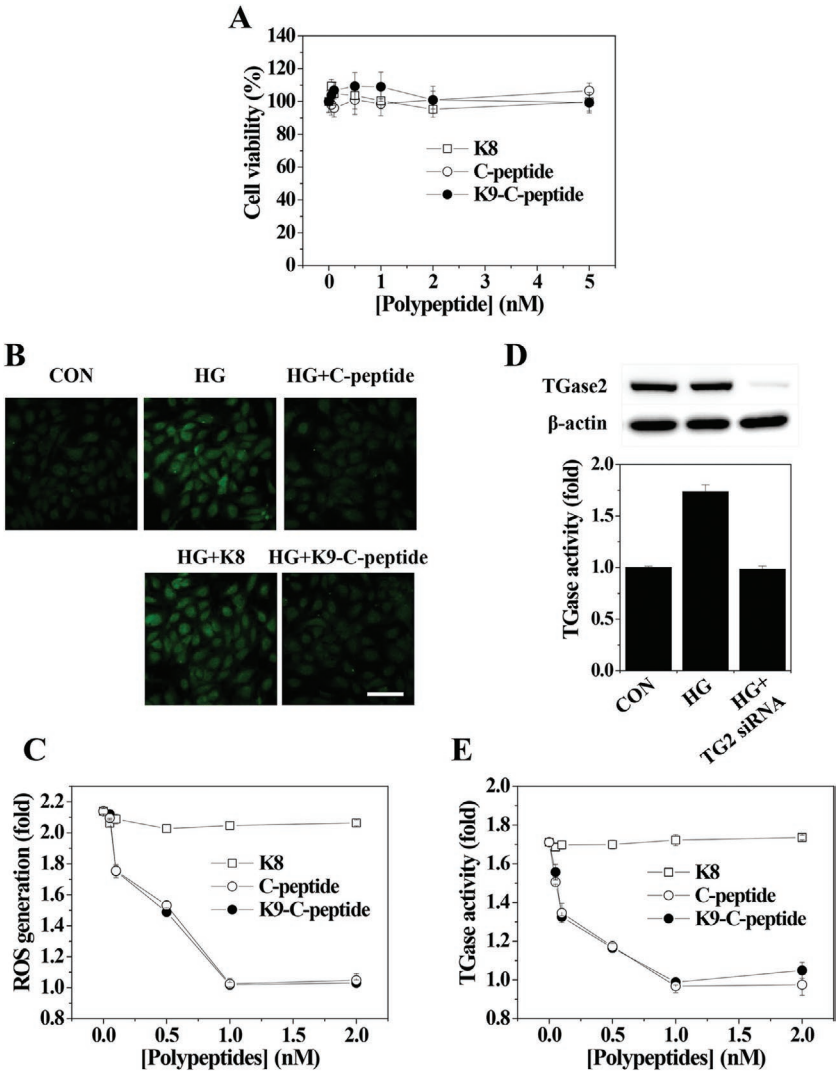

Figure 5. Preventive effect of K9-C-peptide against high glucose-induced ROS generation and TGase2 activation in HAECs. A) HAECs were incubated with the indicated concentrations of K8 or K9-C-peptide for 24 h, and cytotoxicity of the polypeptides was evaluated by MTT assay. B–E) HAECs were incubated with 5 mmol L^{-1} normal glucose (CON) or 30 mmol L^{-1} high glucose (HG) for 3 days in the presence of the B, C, and E) indicated concentrations of K8, human C-peptide, and K9-C-peptide or D) 100 nmol L^{-1} human TGase2 siRNA. Intracellular ROS levels (B and C) and in situ TGase activity (D and E) were determined by confocal microscopy. B) Representative images of intracellular ROS. Scale bar, 100 μm. C) Effects of three polypeptides on HG-induced ROS generation. D) TGase2 siRNA inhibition of HG-induced in situ TGase activity. Expression of TGase protein was determined by Western blot. E) Effect of three polypeptides on HG-induced TGase activity (n = 3). Results are expressed as the mean ± SD from three independent experiments.

a K9-C-peptide conjugate, which has a transition temperature below body temperature. Degradation of K9-C-peptide hydrogel increased depending on the concentrations of four proteases, enzymatic reaction time, and number of protease treatments. We found that K9-C-peptide exerted preventive effects against hyperglycemia-induced ROS generation, TGase2 activation, and apoptosis in aortic endothelial cells. Thus, fusion of C-peptide with ELP polymer could be a useful and cost-effective approach for the sustained delivery of C-peptide to prevent diabetic vascular dysfunction.

ELPs were selected as a genetic fusion scaffold for improved stability and synthetic processes of C-peptide. To use ELPs as macromolecular carriers for improved pharmacokinetics and increase the half-life of ELP fusion, their transition temperature should be tuned to be above body temperature to prevent coacervation in the physiological condition.[32] By contrast, to provide a gel-like depot for sustained local delivery of therapeutic ELP fusion, the transition temperature should carefully tuned to be in the range between injectable temperature in a soluble form and body temperature.[32] In this study, we designed a K9-C-peptide to provide a transition temperature between injectable temperature and body temperature, as it is well known that transition temperatures of ELP V72, V96, and V120 at 25 μmol L^{-1} are 33.2, 31.9, and 28.5 °C, respectively.[33–35] We successfully obtained pure K9-C-peptide with a yield of 10 mg L^{-1} culture by chromatography-free ITC, which had a transition temperature of 31.4 °C at 25 μmol L^{-1}, which is slightly higher than expected from previous reports.[33,34] One possible explanation is that hydrophilic C-peptide fused to the ELP scaffold may interfere with coacervation of K9-C-peptide. We adopted valine and lysine residue in the site of guest residue X at a ratio of 12:1 to conjugate with a fluorophore and form a stable gel when administering into the body because addition of lysine residue enables site-specific amine coupling or crosslinking reactions.

Drug release from implanted hydrogel depots is increased by swelling, erosion, and/or enzymatic degradation of polymer scaffold.[36] Thus, evaluation of hydrogel degradation depending on environmental conditions, including pH, ionic strength, and/or protease concentration near the implantation site, is important for simulation of drug release. In this study, we evaluated the degradation rate of K9-C-peptide hydrogel by on-chip degradation assay, which provides multiplexing capability and reduced reaction time with very small amounts of samples.[27] All four proteases, including collagenase-2, elastase-2, pepsin, and trypsin, have cleavage sites against the elastin motif and increased K9-C-peptide degradation in a concentration-dependent manner. The resulting EC_{50} values of collagenase-2 and elastase-2 were hundreds of times lower than those of the other proteases. To simulate drug release from the hydrogel depot by proteases in blood, elastase-2 was selected because it cleaved elastin strands with higher efficiency than the other proteases. K9-C-peptide degradation increased depending on enzymatic reaction time and number of elastase-2 treatments. In particular, 89.7 ± 0.2% of the hydrogel was degraded after the fifth treatment of elastase-2, whereas 27.9 ± 2.5% of

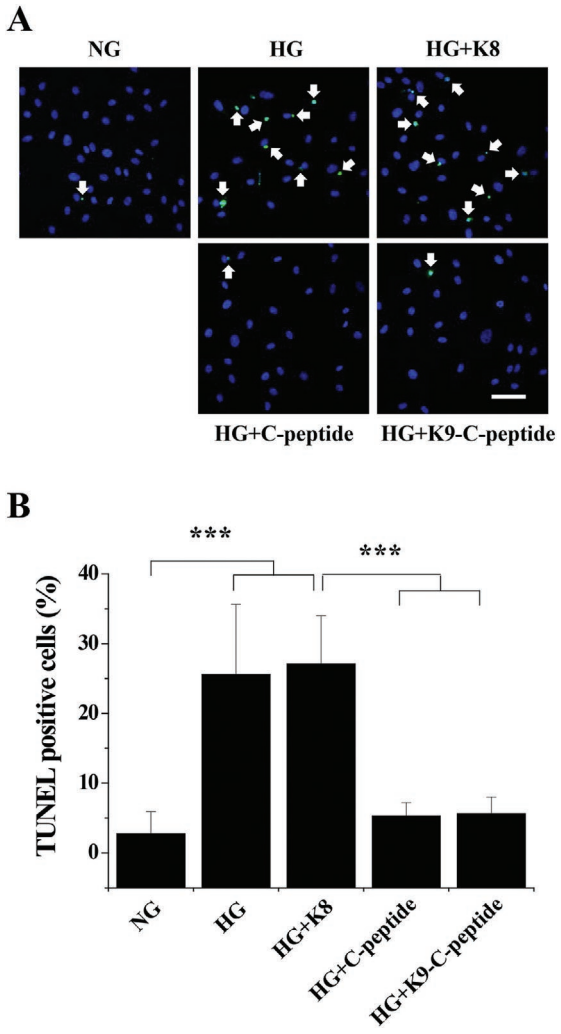

Figure 6. Preventive effect of K9-C-peptide against high glucose-induced apoptosis in HAECs. HAECs were incubated with 5 mmol L^{-1} normal glucose (NG) or 30 mmol L^{-1} high glucose (HG) for 3 days in the presence of 1 nmol L^{-1} K8, human C-peptide, or K9-C-peptide. A) Apoptotic cells (green, indicated by arrows) were stained by TUNEL with nuclear counterstaining using PI (blue) and visualized by confocal microscopy. B) The number of apoptotic cells ($n = 3$) is displayed as a bar graph. Scale bar, 50 μm. Results are expressed as the mean ± SD from three independent experiments. ***$p < 0.001$.

the hydrogel was degraded after the fifth treatment of reaction buffer. These results suggest that K9-C-peptide depot could be slowly degraded through swelling and/or erosion by body fluids and quickly degraded through continuous enzymatic reaction by blood-circulating proteases, including elastase-2 existing in human blood. Further, continuous enzymatic degradation of K9-C-peptide by proteases would be helpful for the clearance of polymer from the body after use as a drug depot.

We also investigated the therapeutic potential of K9-C-peptide against hyperglycemia-induced aortic endothelial dysfunction in HAECs. Chronic hyperglycemia in diabetes mellitus leads to vasculopathy caused by apoptosis of aortic endothelial cells via elevated intracellular ROS and TGase2 activation.[1,2] We found that K9-C-peptide had preventive effects against high glucose-induced ROS generation and TGase2 activation. Furthermore, K9-C-peptide inhibited high glucose-induced apoptosis of HAECs. These results indicate that K9-C-peptide is a potential drug for treating diabetic vasculopathy. We further investigated the possibility that K9-C-peptide has therapeutic potential against other diabetic complications, including diabetic retinopathy, by assessing its preventive effect against vascular endothelial growth factor (VEGF)-induced intracellular events in HAECs. We found that K9-C-peptide prevented VEGF-induced ROS generation and TGase2 activation, with a maximal effect at 1 nmol L^{-1} (data not shown). Thus, K9-C-peptide is a potential drug for treating diabetic complications caused by hyperglycemia and/or VEGF.

Proinsulin C-peptide in physiological concentrations has beneficial effects against diverse diabetic complications in type 1 diabetes animal models.[2,7,10] C-peptide supplementation prevents hyperglycemia-induced vascular damage by activating AMPKα and inhibiting ROS generation, TGase2 activation, and mitochondrial dysfunction.[2,6,8,11] C-peptide replacement normalizes glomerular functions and secretion of urinary albumin in type 1 diabetes patients and animal models.[4,10] C-peptide supplementation also improves diabetic peripheral neuropathy by restoring impaired nerve Na^+/K^+-ATPase activity and diminished NO availability.[10] However, in clinical trials, increased costs due to its relatively short half-life and the lack of effective synthetic methods other than chemical synthesis impede the utilization of C-peptide as peptide drug.[14] To address these limitations, we genetically fused C-peptide with thermosensitive lysine-containing ELPs. We found that K9-C-peptide had similar preventive effects as human C-peptide against high glucose-induced ROS generation, TGase2 activation, and apoptosis. These results indicate that genetic fusion of C-peptide with ELPs does not inhibit the biological activity of C-peptide, thus K9-C-peptide is a potential drug depot for the sustained delivery of C-peptide to prevent diabetic complications.

5. Conclusion

In conclusion, we generated a biocompatible and thermosensitive biopolymer-C-peptide conjugate for treating high glucose-induced aortic endothelial dysfunction. Through recombinant DNA technology, *E. coli* expression, and ITC, we successfully prepared K9-C-peptide with a transition temperature of 28.1 °C at 100 μmol L^{-1}. K9-C-peptide hydrogel formed by sol-gel transition degraded depending on the concentrations of four cleavage enzymes, enzymatic reaction time, and number of enzyme treatments. Furthermore, K9-C-peptide had preventive effects against high glucose-induced intracellular ROS generation, TGase2 activation, and apoptosis. Thus, this biopolymer-C-peptide conjugate has therapeutic potential to treat hyperglycemia-induced vasculopathy and to serve as a drug depot enabling sustained delivery of C-peptide.

Acknowledgements

This work was partially supported by grants from the National Research Foundation of Korea (2015R1A4A1038666 and 2016R1A2A1A05004975 to KSH).

Conflict of Interest

The authors declare no conflict of interest.

Keywords

C-peptide, elastin-like polypeptide, high glucose, human aortic endothelial cells, K9-C-peptide

Received: April 13, 2019
Revised: May 31, 2019
Published online:

[1] M. P. Bhatt, Y. C. Lim, K. S. Ha, *Cardiovasc. Res.* **2014**, *104*, 234.
[2] M. P. Bhatt, Y. C. Lim, J. Hwang, S. Na, Y. M. Kim, K. S. Ha, *Diabetes* **2013**, *62*, 243.
[3] A. Ceriello, M. A. Ihnat, J. E. Thorpe, *J. Clin. Endocrinol. Metab.* **2009**, *94*, 410.
[4] C. E. Hills, N. J. Brunskill, P. E. Squires, *Am. J. Nephrol.* **2010**, *31*, 389.
[5] Y. Ido, A. Vindigni, K. Chang, L. Stramm, R. Chance, W. F. Heath, R. D. DiMarchi, E. Di Cera, J. R. Williamson, *Science* **1997**, *277*, 563.
[6] Y. C. Lim, M. P. Bhatt, M. H. Kwon, D. Park, S. Lee, J. Choe, J. Hwang, Y. M. Kim, K. S. Ha, *Cardiovasc. Res.* **2014**, *101*, 155.
[7] Y. C. Lim, M. P. Bhatt, M. H. Kwon, D. Park, S. Na, Y. M. Kim, K. S. Ha, *J. Invest. Dermatol.* **2015**, *135*, 269.
[8] M. P. Bhatt, Y. C. Lim, Y. M. Kim, K. S. Ha, *Diabetes* **2013**, *62*, 3851.
[9] H. Y. Jeon, Y. J. Lee, Y. S. Kim, S. Y. Kim, E. T. Han, W. S. Park, S. H. Hong, Y. M. Kim, K. S. Ha, *FASEB J.* **2019**, *33*, 750.
[10] J. Wahren, A. Kallas, A. A. Sima, *Diabetes* **2012**, *61*, 761.
[11] Y. J. Lee, S. H. Jung, S. H. Kim, M. S. Kim, S. Lee, J. Hwang, S. Y. Kim, Y. M. Kim, K. S. Ha, *Diabetes* **2016**, *65*, 2414.
[12] J. P. Ashby, B. M. Frier, *Ann. Clin. Biochem.: An Int. J. Biochem. Lab. Med.* **1981**, *18*, 125.
[13] J. Wahren, H. Foyt, M. Daniels, J. C. Arezzo, *Diabetes Care* **2016**, *39*, 596.
[14] C. G. Jolivalt, M. Rodriguez, J. Wahren, N. A. Calcutt, *Diabetes, Obes. Metab.* **2015**, *17*, 781.
[15] S. Banskota, P. Yousefpour, N. Kirmani, X. Li, A. Chilkoti, *Biomaterials* **2019**, *192*, 475.
[16] J. R. McDaniel, D. J. Callahan, A. Chilkoti, *Adv. Drug Delivery Rev.* **2010**, *62*, 1456.
[17] S. R. MacEwan, A. Chilkoti, *J. Controlled Release* **2014**, *190*, 314.
[18] C. A. Gilroy, S. Roberts, A. Chilkoti, *J. Controlled Release* **2018**, *277*, 154.
[19] J. A. MacKay, M. N. Chen, J. R. McDaniel, W. G. Liu, A. J. Simnick, A. Chilkoti, *Nat. Mater.* **2009**, *8*, 993.
[20] M. Amiram, K. M. Luginbuhl, X. Li, M. N. Feinglos, A. Chilkoti, *J. Controlled Release* **2013**, *172*, 144.
[21] H. Betre, W. Liu, M. R. Zalutsky, A. Chilkoti, V. B. Kraus, L. A. Setton, *J. Controlled Release* **2006**, *115*, 175.
[22] S. M. Sinclair, J. Bhattacharyya, J. R. McDaniel, D. M. Gooden, R. Gopalaswamy, A. Chilkoti, L. A. Setton, *J. Controlled Release* **2013**, *171*, 38.
[23] G. Qin, P. M. Perez, C. E. Mills, B. D. Olsen, *Biomacromolecules* **2016**, *17*, 928.
[24] J. W. Jung, S. H. Jung, J. O. Yoo, I. B. Suh, Y. M. Kim, K. S. Ha, *Biosens. Bioelectron.* **2009**, *24*, 1469.
[25] D. H. Kong, S. H. Jung, H. Y. Jeon, W. J. Kim, Y. M. Kim, K. S. Ha, *Analyst* **2015**, *140*, 6588.
[26] S. H. Kim, S. H. Jung, D. H. Kong, H. Y. Jeon, M. S. Kim, E. T. Han, W. S. Park, S. H. Hong, Y. M. Kim, K. S. Ha, *Clin. Biochem.* **2016**, *49*, 127.
[27] H. Y. Jeon, S. H. Jung, Y. M. Jung, Y. M. Kim, H. Ghandehari, K. S. Ha, *Anal. Chem.* **2016**, *88*, 5398.
[28] A. A. Aimetti, M. W. Tibbitt, K. S. Anseth, *Biomacromolecules* **2009**, *10*, 1484.
[29] M. Kato, K. Sakai-Kato, H. Jin, K. Kubota, H. Miyano, T. Toyo'oka, M. T. Dulay, R. N. Zare, *Anal. Chem.* **2004**, *76*, 1896.
[30] J. V. Olsen, S. E. Ong, M. Mann, *Mol. Cell. Proteomics* **2004**, *3*, 608.
[31] T. S. Thring, P. Hili, D. P. Naughton, *BMC Complementary Altern. Med.* **2009**, *9*, 27.
[32] W. Hassouneh, S. R. MacEwan, A. Chilkoti, *Methods Enzymol.* **2012**, *502*, 215.
[33] M. Shah, P. Y. Hsueh, G. Sun, H. Y. Chang, S. M. Janib, J. A. MacKay, *Protein Sci.* **2012**, *21*, 743.
[34] J. Dhandhukia, I. Weitzhandler, W. Wang, J. A. MacKay, *Biomacromolecules* **2013**, *14*, 976.
[35] Y. H. Cho, Y. J. Zhang, T. Christensen, L. B. Sagle, A. Chilkoti, P. S. Cremer, *J. Phys. Chem. B* **2008**, *112*, 13765.
[36] Y. Luo, K. R. Kirker, G. D. Prestwich, *J. Controlled Release* **2000**, *69*, 169.

